JOURNAL OF SOLID STATE CHEMISTRY 5, 369–381 (1972)

The High Temperature Defect Equilibria of CdSe

W. D. CALLISTER, JR., C. F. VAROTTO* AND D. A. STEVENSON

Department of Materials Science and Engineering, Stanford University, Stanford, California 94305

Received November 25, 1971

The high temperature defect equilibria of CdSe have been investigated by measuring the electrical transport properties as a function of component pressure and temperature under equilibrium conditions. Measurements were performed on undoped, Cu- and In-doped single crystals.

The electron concentration for undoped CdSe varies as

$$n \propto P_{Cd}^{1/3}$$

at temperatures between 650 and 850°C and in Cd-rich vapor. A dominant doubly ionized native donor, either a Cd interstitial or Se vacancy, is proposed to explain this behavior with an incorporation energy for this defect of 1.90 eV. A lower value for the Cd pressure exponent is observed for In- and Cu-doped CdSe, and also for undoped CdSe at lower temperatures. It is proposed that these doping elements behave as donors under the experimental conditions and that residual donor impurities exist in the undoped CdSe. Measurements of the Hall mobility of the charge carriers and the relaxation time for the conductivity change are also reported and compared with theory.

Introduction

The electrical and optical properties of the II–VI semiconducting compounds are strongly dependent on the type and concentration of point defects which are present. In order to better understand the point defect structure in CdSe, we have measured the high temperature electrical transport properties, conductivity and Hall mobility, as functions of temperature and component pressure at equilibrium conditions. Other investigations (*1–3*), have examined the electrically active defect structures after equilibration at high temperature and measurement near room temperature and below following a rapid quench. Comparison between measurements made at temperatures under equilibrium conditions and after quenching provides insight concerning the effectiveness in retaining the defect structure upon cooling. Chemical diffusion coefficients may be measured at the annealing temperature by measurement of the conductivity response time of the material after imposing a stepwise change in chemical potential (*4*). Comparison is made of the defect models implied from the present electrical property measurements with those implied from self-diffusion studies to establish if they are mutually compatible.

Experimental Methods

Source and Preparation of Samples

Single crystalline material for this study was obtained from several sources; the growth techniques and impurity concentrations from emission spectrographic analyses are included in Table I. The electrical properties of hexagonal CdSe are nearly isotropic (*5*); consequently, crystallographic orientation of the specimens was not a consideration. The rectangular parallelepiped samples, with approximate dimensions of $1.5 \times 2.5 \times 14$ mm^3, were etched to remove surface contamination prior to insertion into the experimental apparatus.

General Features of the Apparatus

The high-temperature measuring apparatus was an extension of designs described in the

* Fellow, Consejo Nacional de Investigaciones, Cientificas y Technicas, Argentina. Present address: Centro Atomico, S.C. de Bariloche (R.N.) Argentina.

TABLE I

SOURCES AND IMPURITY ANALYSES ON CdSe SAMPLES WHICH WERE USED IN THIS STUDY

Sample designation	Source	Dopant	Concns of impurities detected in the As-Grown material (cm^{-3})						
			Ag	Cu	Fe	In	Mg	Te	Zn
01CS	CMR[a]	Undoped	4.8×10^{15}	1.4×10^{16}	4.3×10^{16}	ND	7.1×10^{16}	ND	1.6×10^{17}
02CS	Burmeister[b]	Undoped	4.8×10^{15}	1.9×10^{17}	$<3.1 \times 10^{16}$	ND	7.1×10^{15}	ND	1.6×10^{17}
03CS	Clevite[c]	Undoped	4.8×10^{15}	4.1×10^{17}	$<3.1 \times 10^{16}$	ND	1.4×10^{16}	ND	1.1×10^{17}
04CS	Clevite[cd]	In	4.8×10^{15}	8.2×10^{16}	3.1×10^{16}	7.5×10^{17}	$<7.1 \times 10^{15}$	ND	6.6×10^{18}
05CS	Clevite[cd]	Cu	4.8×10^{15}	8.2×10^{17}	$<3.1 \times 10^{16}$	ND	1.1×10^{16}	ND	5.3×10^{16}
07CS	Clevite[c]	Undoped	4.8×10^{15}	4.1×10^{17}	$<3.1 \times 10^{16}$	ND	1.4×10^{16}	ND	1.1×10^{17}

[a] Stanford Center for Materials Research; doubly sublimed CdSe powder and vertical Bridgman technique.
[b] Grown by Bridgman technique.
[c] Grown from the vapor phase by a slightly modified variation of the method described by Greene et al. (*18*).
[d] In added during growth by vapor transport from In_2S_3 source.
[e] Cu added as Cu_2Se and sintered with the polycrystalline CdSe prior to growth.

literature (*6–7*) and is illustrated schematically in Fig. 1. A two-zone nichrome-wound furnace was employed which permitted independent control of both component vapor pressure and sample temperature; a schematic temperature profile is included in the figure. The vapor and reflux chamber (D) was constructed of quartz tubing and its upper extremity was attached to a quartz-to-stainless-steel junction which in turn was welded to the stainless-steel manifold. The inside of the chamber was coated with a thin graphite layer to aid the refluxing process. The lower extremity of the quartz tube was closed to form the vapor element reservoir (A); a small 1/4 in. thermocouple well (B) allowed measurement of the reservoir temperature. Approximately 25 g of high purity Cd shot were used in the reservoir. The manifold assembly (L) provided for attachment of the following items to the vapor and reflux chamber: an aneroid pressure gauge (P) a thermocouple pressure gauge (Q) an adsorption cryopump (V) a source of high purity argon (Z) and the sample holder assembly (C). The component parts were attached with vacuum-tight flanges and crushable Cu gaskets.

Sample Holder Assembly

The sample holder assembly, illustrated in Fig. 2, was constructed entirely of quartz except for the wire leads and thermocouple. It consists of a backing plate (G) which is attached to the holder support tube (H); the upper end of the support tube extends into a quartz-to-stainless-steel junction which is welded to the holder

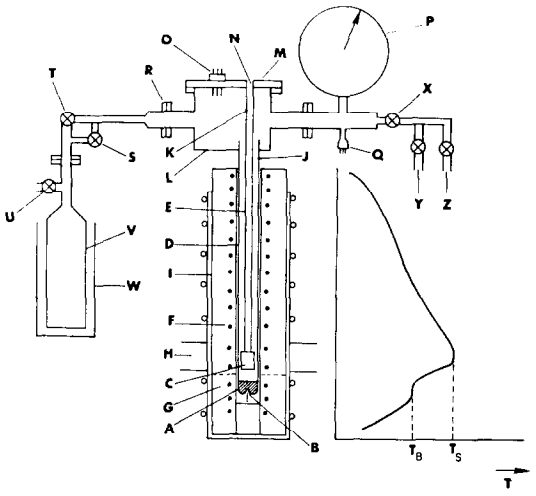

FIG. 1. Schematic diagram of the apparatus for measuring high-temperature transport properties under specified equilibrium conditions. (A) Vapor element reservoir; (B) reservoir thermocouple; (C) sample holder; (D) vapor and reflux chamber; (E) holder support tube; (F) furnace (upper zone); (G) furnace (bottom zone); (H) magnet pole piece; (I) copper heat shield (water cooled); (J) stainless-steel to quartz junction (vapor reflux chamber); (K) stainless-steel to quartz junction (holder support tube); (L) manifold assembly (stainless-steel); (M) sample holder flange; (N) thermocouple feed-through; (O) electrical feed-through; (P) aneroid gauge (0–800 Torr); (Q) thermocouple pressure gauge; (R) crushable gasket flanges; (S) needle bypass valve; (T) evacuation valve; (U) pump exhaust valve; (V) adsorption cryopump; (W) liquid nitrogen Dewar; (X) inlet valve-fine control; (Y) auxiliary inlet or evacuation line; (Z) inlet line (high purity argon); (T_B) bath temperature; (T_S) sample temperature; $T_S > T_B$; $T_B > T_M$ of element.

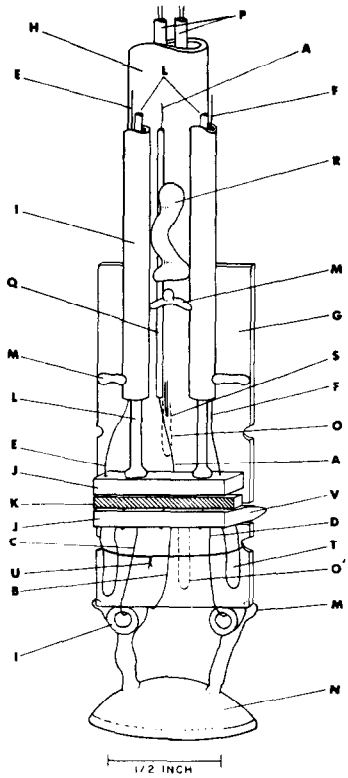

FIG. 2. Schematic diagram of the 6-probe sample holder. (A) Hall electrode and lead; (B) Hall electrode; (C) voltage electrode; (D) voltage electrode; (E) current electrode; (F) current electrode; (G) quartz backing plate; (H) quartz holder support tube; (I) quartz lead insulator tube; (J) quartz sample holder plate; (K) sample; (L) quartz spring load transmittance rods; (M) attachment points for insulator tubes; (N) quartz protection cup; (O & O') capillary thermocouple tubes (extensions of holder support tube); (P) thermocouples; (Q) capillary lead insulator tube; (R) attachment between holder support tube and backing plate; (S) thermocouple bead; (T) support leg for sample plate; (U) attachment wire; (V) alignment post for sample plate.

flange assembly (M) of Fig. 1. The sample (K) is sandwiched and spring-loaded between two small quartz plates (J); the tungsten-coiled springs are located in a cooler region of the furnace and the load is transmitted to the top plate by means of quartz rods (L) which run through the electrical insulator tubes (I). The lower plate is held firmly in position on the backing plate by means of two alignment posts (V) and two support legs (T). The electrical contacts of 0.004 in. Mo wire run between the sample and quartz plates; the extensions of the contacts serve as the electrical leads. Since the distance between the sample and bath surface is only about 2 in., the protection cup (N) was installed to protect the sample from any small droplets which may be expelled from the boiling bath, and also to reduce the vapor convection currents in the sample region. The lower extremity of the holder support tube was drawn into two capillary thermocouple tubes (O and O') with the latter being approximately 1 cm behind the former which is in contact with the back of the backing plate.

Refluxing Technique

The vapor pressure of the elemental components was varied and controlled using a refluxing method described by Van Doorn (*7*). The refluxing apparatus operates similar to that in a vapor diffusion pump. The liquid reservoir is placed in a state of boiling by adjustment of the reservoir temperature and the imposed Ar pressure. The liquid vaporizes at the bath surface and rises up the reflux chamber past the sample to a region where the temperature is the same as the reservoir. At this point the metallic vapor condenses into small liquid droplets on the graphite-coated wall and rolls down the wall to a hotter region where revaporization occurs. The refluxing action is the steady circulation of droplets down the wall and vapor up the center of the chamber. This reflux region separates the pure metal vapor in the lower chamber from the pure Argon in the upper, cooler regions; there is a mixture of vapors somewhere in between.

Conductivity and Hall Measurements

Conductivity and Hall measurements were made with a constant dc current of approximately 10 mA passing through the sample; a bucking potential was used to null out Seebeck voltages. The electrical contacts were checked for ohmic behavior by making a V–I trace at all temperatures. An electromagnet with a pole-piece separation of 3.5 in. provided magnetic fields of 4.5 kG. By reversing the polarity of the field with the current flow in both directions and averaging the four readings, the Hall signal was corrected for Nernst voltages and any electrode misalignment. At higher temperatures Nernst voltages were significant.

Results

For a bulk sample to respond to a change in experimental conditions of temperature and

pressure, a finite time is required. Smith (*8*) made high-temperature electrical transport measurements on CdSe and reported an exponential time dependence for equilibration, with an associated relaxation time. He reported the relaxation time to be temperature dependent, with a value for a 1-mm thick sample at 660°C of approximately 30 min. However, in our investigation of samples 1.5-mm thick, the time necessary for the sample to achieve equilibrium after a change in temperature or pressure at all temperatures was less than 1 min. At 660°C a relaxation time of 16 sec was measured which is approximately two orders of magnitude faster than Smith's value. The following data represent values measured after waiting a period at least as long as his reported relaxation times.

In order to confirm that equilibrium is attained very rapidly, a specimen (sample 07CS) was annealed at a constant temperature and Cd pressure for over 400 hr. The conductivity was measured as a function of time and no change was observed after the initial measurement taken immediately after bringing the system to the desired temperature and pressure. Therefore, it was concluded that the states represented by the short relaxation times are indeed equilibrium ones.

Hall mobility measurements were made as a function of both Cd vapor pressure and temperature and no pressure dependence was observed. Figure 3 shows the temperature dependence of the Hall mobility for several CdSe samples with different doping levels; *n*-type behavior was observed in all cases. It appears that above 450°C the mobility was independent of impurity content; however, below this temperature there was a substantial decrease in mobility for the In-doped sample.

Figure 4 represents the variation of the electron concentration with Cd vapor pressure at several temperatures for an undoped CdSe sample. The relationship between electron concentration *n*

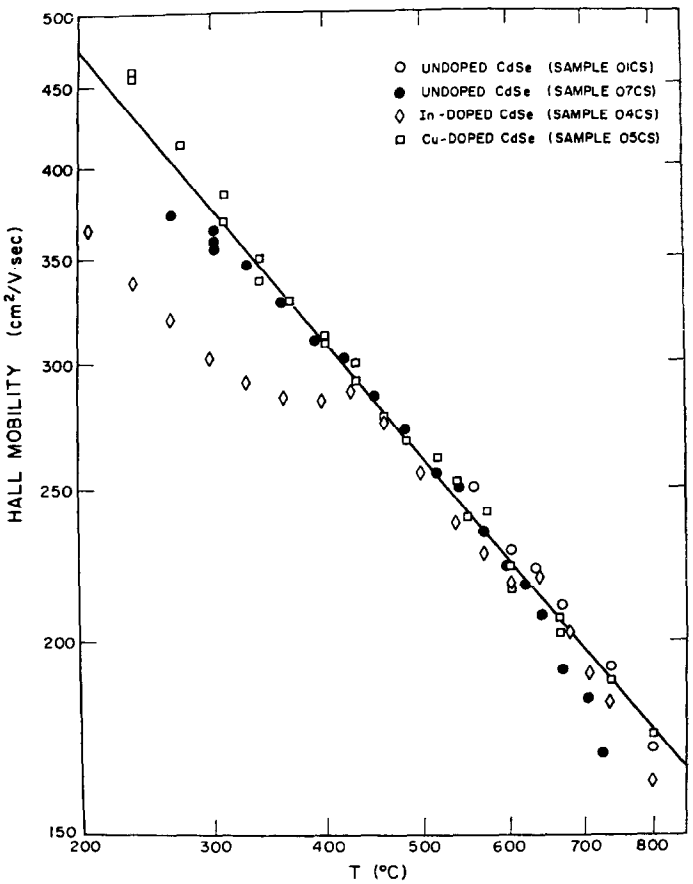

FIG. 3. The temperature dependence of the Hall mobility in undoped, Cu- and In-doped CdSe.

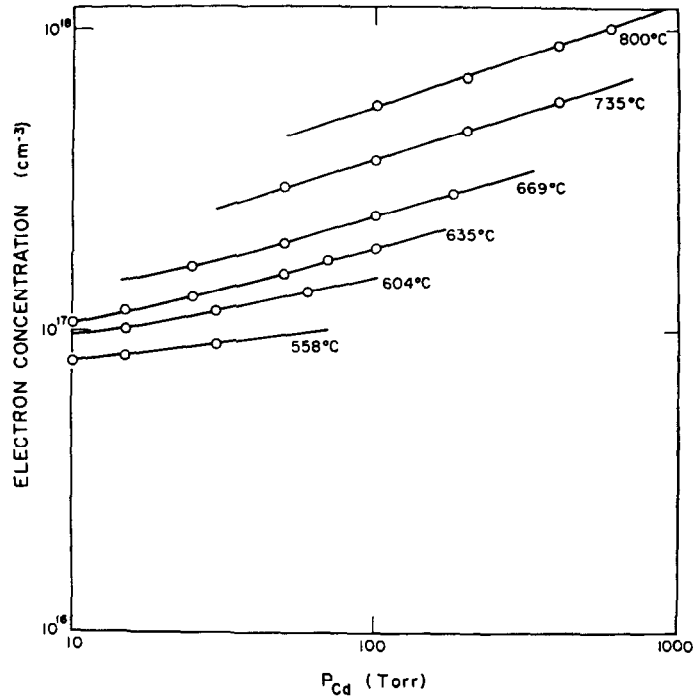

FIG. 4. The equilibrium electron concentration of undoped CdSe (sample 01CS) as a function of the Cd vapor pressure at fixed temperatures.

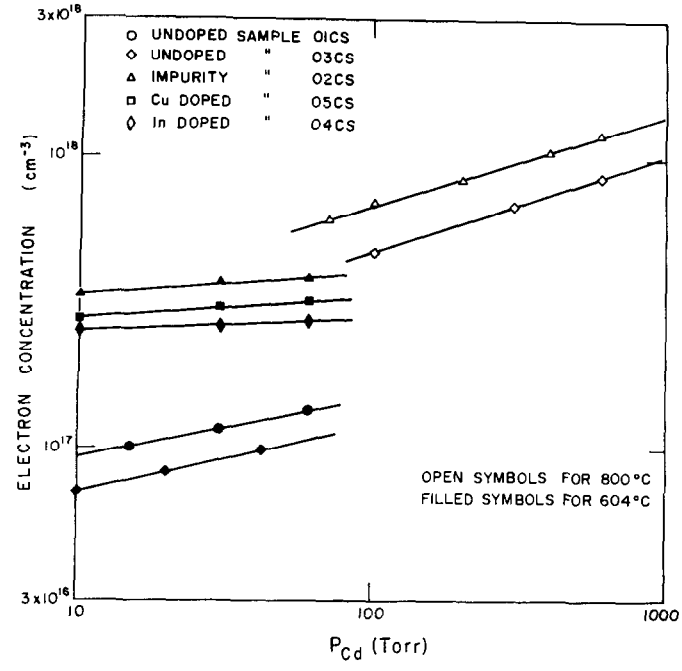

FIG. 5. The equilibrium electron concentration as a function of Cd vapor pressure for doped and undoped CdSe samples at 604 and 800°C.

and Cd pressure P_{Cd} may be described mathematically as

$$n \propto P_{Cd}^{\gamma}, \tag{1}$$

where the pressure exponent γ takes on a value of 1/3 for temperatures above 650°C. At temperatures lower than this, some curvature appears, the slopes decrease, and finally at temperatures below 600°C the electron concentration becomes almost independent of pressure.

Similar measurements were made on Cu- and In-doped samples which indicated that both impurities acted as donors at elevated temperatures with a substantial increase in electron concentration over the undoped samples, especially at the lower temperatures. This is illustrated in Fig. 5 which shows the pressure dependence of the electron concentration for all five samples at two characteristic temperatures. At 800°C, only the data points for the two samples with extreme values are included to avoid confusion.

Discussion

High Temperature Defect Equilibria

The experimental results for the high-temperature electrical behavior illustrated in Fig. 4, indicate that there is an increase of electron concentration with Cd vapor pressure. The nature of the native disorder may be implied from the exact pressure dependence of the electron concentration.

The incorporation and subsequent ionization of Cd interstitials may be described by the following quasi-chemical defect reaction and associated mass action expression:

$$Cd(g) \leftrightarrows Cd_i^{\cdot\cdot} + 2e'; \tag{2}$$

$$K_{Cd_i} = \frac{[Cd_i^{\cdot\cdot}]n^2}{P_{Cd}}. \tag{3}$$

The assumption that the electroneutrality condition may be approximated by dominance of electrons and doubly ionized Cd interstitials,

$$n = 2[Cd_i^{\cdot\cdot}], \tag{4}$$

leads to

$$n = 2[Cd_i^{\cdot\cdot}] = (2K_{Cd_i})^{1/3} P_{Cd}^{1/3}. \tag{5}$$

Hence, for a given temperature, a plot of the logarithm of the electron concentration versus the logarithm of the Cd partial pressure should yield a slope of 1/3 if the crystal charge neutrality condition is correctly described by Eq. (4). The same dependence on Cd pressure for the electron concentration results for the incorporation of a doubly ionized Se vacancy if the electroneutrality condition is approximated by

$$n = 2[V_{Se}^{\cdot\cdot}]. \tag{6}$$

The former charge neutrality condition will be assumed for the subsequent discussion. At temperatures greater than 650°C in undoped CdSe, Fig. 4, the vapor pressure dependence of the electron concentration is described by

$$n \propto P_{Cd}^{1/3}. \tag{7}$$

It is concluded that doubly ionized native donors, either Cd interstitials or Se vacancies, are the dominant electrically active defects in this temperature range. The same relationship between electron concentration and Cd pressure was observed by Smith (*8*) between temperatures of 950 and 1250°K. He concurred with the proposed defect model and, in addition, there was good agreement concerning the magnitude of the electron concentrations.

Influence of Impurity Donors

At temperatures below 650°C for undoped CdSe (Fig. 4), the pressure exponent tends to decrease with decreasing temperature, until at 558°C the electron concentration becomes almost Cd pressure independent. This behavior is assumed to be due to the presence of residual electrically active foreign donor impurities with concentrations comparable to the native defect concentrations at these temperatures. Therefore, the electroneutrality condition, Eq. (4), is modified to read:

$$2[Cd_i^{\cdot\cdot}] + [D^{\cdot}] = n, \tag{8}$$

where $[D^{\cdot}]$ is the concentration of ionized foreign donors, assumed to be singly ionized. Substituting $[Cd_i^{\cdot\cdot}]$ from Eq. (3) into Eq. (8) yields

$$\frac{(2K_{Cd_i})P_{Cd}}{n^2} + [D^{\cdot}] = n. \tag{9}$$

Simultaneous solution for K_{Cd_i} and $[D^{\cdot}]$ from Eq. (9) is possible for two different pressures at a constant temperature since both n and P_{Cd} are known. Figure 6 represents the dependence of K_{Cd_i} on reciprocal temperature for two undoped samples. The slope of the parallel lines through the two sets of data points yields an activation energy of 1.90 eV; this corresponds to the standard enthalpy of incorporation of Cd vapor to form a doubly ionized cadmium interstitial, in accordance with Eq. (2). This corresponds favorably with the value of 1.90 eV reported by

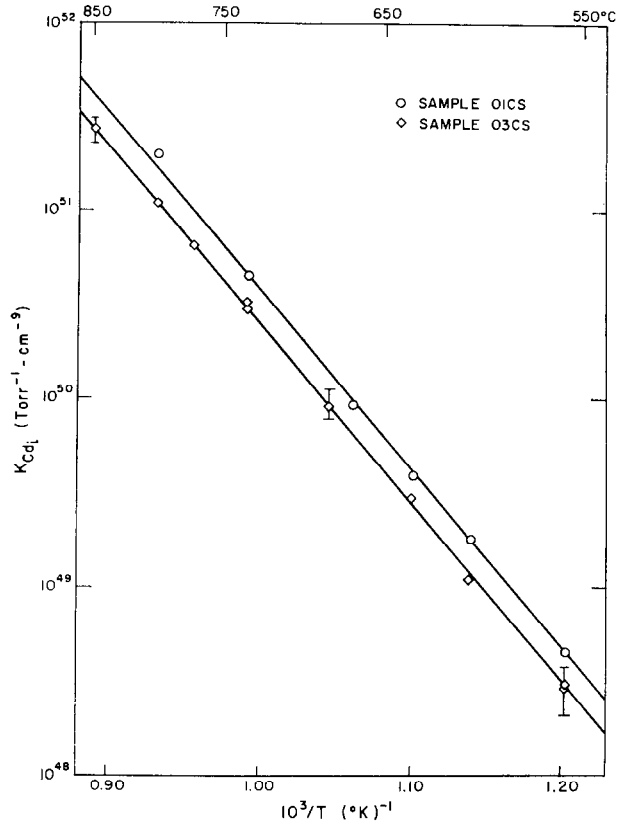

FIG. 6. The temperature dependence of the incorporation constant for doubly ionized native donors in undoped CdSe.

Smith (*8*) for undoped samples measured at temperatures greater than 680°C. The constant and slight difference in the logarithm of the absolute magnitude of K_{Cd_i} with temperature for the two samples in Fig. 6 cannot be explained.

For Cu- and In-doped samples, the pressure exponent tends to lower values beginning at a higher temperature (about 735°C) than for the undoped specimens. This is the expected behavior if the impurities behave as donors, inasmuch as their concentrations become comparable to the native donors at higher temperatures.

The ionized donor concentration, [D˙] from Eq. (9), was computed for all five samples at the various temperatures at which measurements were made. Figure 7 gives values of [D˙] as a function of temperature for the In-doped sample as well as for an undoped one. Measurements were made both upon heating up and cooling, with good agreement. The computed impurity donor concentration of all specimens is temperature independent within the limitation of experimental error.

The high-temperature electrical transport measurements for sample 04CS indicate that In acts as a donor inasmuch as it appears to be the dominant impurity from spectrographic analysis, and the electron concentration is enhanced by its presence. The calculated [D˙] for this sample of 2.6×10^{17} cm^{-3} is intermediate between In concentrations of 7.5×10^{17} and 2.1×10^{16} cm^{-3} determined from emission spectrographic analyses for materials in the as-grown and post-measurement states, respectively. It is therefore concluded from the experimental results that In is a donor at high temperatures and Cd-rich atmospheres in CdSe and may be solvent extracted at a slow rate during annealing. From the high-temperature electrical behavior of the Cu-doped specimen, sample 05CS (Fig. 5), the electron concentration is increased by its presence, as with In described above. A computed donor concentration of 2.9×10^{17} cm^{-3} is in reasonable agreement with the as-grown and postmeasurement Cu concentrations of 8.2×10^{17} and 8.2×10^{16} cm^{-3}, respectively. It appears that the

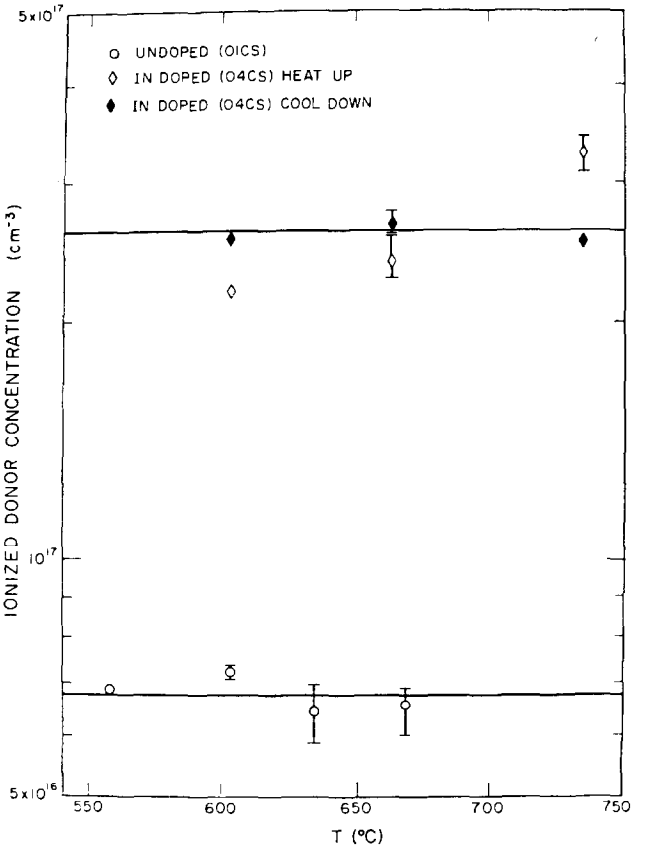

FIG. 7. The ionized foreign donor concentration as a function of temperature of undoped (sample 01CS) and In-doped (sample 04CS) CdSe.

impurity Cu displays donor behavior at elevated temperatures in CdSe. Sample 02CS showed a high concentration of residual donor impurities which is reflected in a computed [D˙] value of 3.3×10^{17} cm^{-3} being larger than that for any of the other samples and greater than the impurity concentrations detected for this sample. Undoped samples 01CS and 03CS appear to have low residual donor impurity levels; the computed donor concentrations are 6.8×10^{16} and 8.8×10^{16} cm^{-3}, respectively, being of the same order as those detected impurities thought to be electrically active.

Comparison of High Temperature Electrically Active and Self-Diffusion Defect Structures

One of the motives for this investigation was to compare the high-temperature defect structures for CdSe as elucidated from high-temperature electrical transport and self-diffusion measurements. Selenium self-diffusion measurements were made by Woodbury and Hall (*9*) between 700 and 1000°C over the complete field of existence. It was proposed that the defect responsible for the Se self-diffusion behavior is a neutral Se interstitial for the Se-rich portion of the phase field, whereas, under high Cd pressures a Se vacancy was proposed as the dominant mobile defect. Borsenberger, Stevenson and Burmeister (*3*) conducted Cd self-diffusion measurements as a function of the Cd vapor pressure at 800°C over the entire existence field, at Cd-saturation between 550 and 878°C, and Se-saturation between 760 and 939°C. The self-diffusion coefficient, D_{Cd}, was observed to vary with Cd vapor pressure according to

$$D_{Cd} \propto P_{Cd}^{0.47}. \tag{10}$$

If the electroneutrality condition is dominated by electrons and singly ionized Cd interstitials, $Cd_i^{\cdot}$,

$$n = [Cd_i^{\cdot}] \tag{11}$$

then

$$[Cd_i^{\cdot}] \propto P_{Cd}^{1/2}. \quad (12)$$

Since the experimental pressure exponent is 1/2, within experimental error, it was concluded that the dominant defect responsible for self-diffusion on the Cd sublattice is a singly ionized Cd interstitial.

The dominant electrically active defects at high temperatures, as suggested by Eqs. (4) or (6), are electrons and doubly ionized native donors, either Cd interstitials or Se vacancies. Clearly, only one of the three electroneutrality conditions Eqs. (4), (6), or (11) can exist at any one time, and therefore, some reconciliation is necessary.

Assuming that self-diffusion of each component may be attributed to a single defect specie, three possibilities exist which may be applied in attempting to explain this disparity: (a) one electroneutrality condition could dominate which is consistent with the electrical behavior, while diffusion is by a minority species; (b) or conversely, the diffusing species could be included in the electroneutrality condition with electrons in minority concentrations; and (c) neither the dominant diffusing defect nor electrons enter into the electroneutrality condition, but two other oppositely charged species dominate.

Explanation on the basis of Case (a) is not possible since for either of the electroneutrality conditions Eqs. (4) and (6), the only Cd pressure exponents permitted for defects on the Cd sublattice, as described in the appendix, are ± 1, $\pm 2/3$, and $\pm 1/3$; a value of $+1/2$, which is consistent with the Cd self-diffusion behavior, is excluded. Cases (b) and (c) are eliminated since an atomic defect on the Cd sublattice with a Cd pressure exponent of $+1/2$ leads to the same exponent for the electron concentration (instead of $+1/3$) for all possible situations, irrespective of whether one or both species enter into the electroneutrality condition. Therefore, reconciliation of self-diffusion and electrical transport models is not possible within the present theoretical framework if it is assumed that self-diffusion is due to a single defect on each component sublattice.

Relaxation Times

Very short periods of time (less than 1 min) are required at high temperatures for CdSe samples to come to steady conductivity values after a change in components pressure (Results); considerably longer equilibration times were reported by Smith (*8*) for samples of similar thickness. Since the results of both investigations are in agreement, this would indicate that both equilibrium states are identical.

The only apparent difference between investigations is the technique employed to control the component vapor pressure in the vicinity of the sample. Smith used a pure Cd bath to supply the vapor at a pressure determined by its temperature, and the system was maintained at a total pressure of 1 atm by a flow of Ar. This may be contrasted to the refluxing technique (described in Refluxing Techniques), in which Ar was essentially excluded from the sample region. It is conceivable that the kinetics of vapor transport or of defect incorporation at the sample interface may be a function of the presence of Ar in the ambient, and therefore some process other than bulk diffusion could be rate limiting. Since the equilibrium results of both investigations are the same, it would seem that the more rapid equilibration times would be indicative of the bulk diffusion process.

For the geometry of samples used, the relaxation time τ may be related to the interdiffusion coefficient, $\tilde{D}_{CdSe}$, by the relation

$$\tilde{D}_{CdSe} \cong \frac{d^2}{\pi^2 \tau} \quad (13)$$

where d is the smallest sample dimension (*10*). At 660°C, $\tilde{D}_{CdSe}$ values of 5.6×10^{-7} and 8.4×10^{-5} cm^2/sec were computed, respectively, from Smith and this investigation, his being approximately two orders of magnitude smaller than ours.

For other of the II–VI compounds, discrepancies exist for interdiffusion coefficients as determined from relaxation times measured at high temperatures. In CdS, Boyn, Goede and Kuschnerus (*11*) report, for Cd-rich atmospheres and at temperatures in the vicinity of 650°C, interdiffusion coefficients which are approximately two orders of magnitude smaller than those measured by Kumar and Kröger (*12*) under the same experimental conditions. For both studies the Cd pressure was controlled by essentially the same technique.

Whelan and Shaw (*13*) found relaxation times for CdTe corresponding to interdiffusion coefficients approximately 20 times greater than those reported by Zanio (*4*) for comparable experimental conditions—temperatures around 700°C and Cd-rich atmospheres. The former investigators

employed the Van Doorn technique to control the pressure, while the latter used a method similar to Smith's (*14*). No explanation can be offered for these disparities in the magnitude of interdiffusion coefficients; for CdTe and CdSe the only difference between investigations is the technique of component pressure control.

Electron Mobilities

The Hall mobilities for CdSe, illustrated in Fig. 3 as a function of temperature, are taken to be electron mobilities since the electron concentrations at all temperatures are at least two orders of magnitude greater than the hole concentrations. No explanation can be given for the lower mobility values for the In-doped sample below 450°C.

Theoretical mobility calculations may be made by reciprocal addition of contributions to the mobility by polar scattering by longitudinal optical modes, deformation potential scattering by acoustic modes, piezoelectric scattering by acoustic modes, and by ionized impurity scattering. The contributions from these latter two mechanisms are neglected inasmuch as scattering by ionized impurities in materials with moderate impurity levels is normally significant only at room temperature and below, and piezoelectric scattering amounts to at most a 1% correction above 300°C.

Theoretical expressions for polar optical mode and deformation potential scattering are taken from Howarth and Sondheimer (*15*) and Bardeen and Shockley (*16*), respectively, while values of the parameters for CdSe are given by Burmeister and Stevenson (*5*). Figure 8 presents optical, acoustic and total theoretical mobilities, as a function of temperature and also experimental values from this investigation. Since values for the deformation potential in the acoustic mode scattering expression could not be found

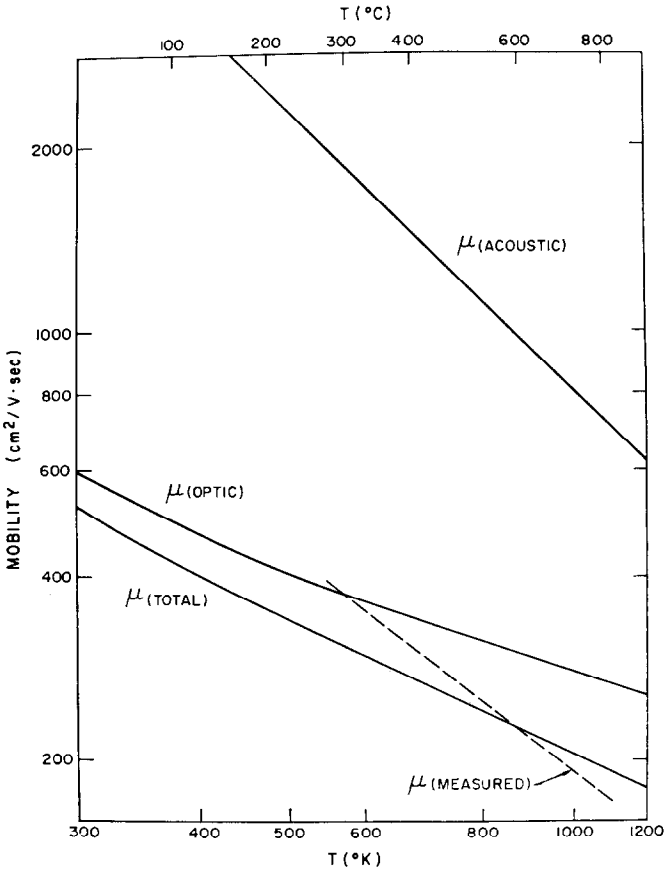

FIG. 8. The temperature dependence of theoretical optical and acoustic contributions, total, and measured Hall mobilities for CdSe.

in the literature, it was estimated to be 12 eV on the basis of the experimental mobilities. Optical mode scattering appears to dominate over the temperature range of interest, and agreement between measured and computed total mobilities is fair.

Comparison Between Equilibrium and Quenched-In Electrical Properties and Defect Structures

By comparison of electrical behavior at actual equilibrium high-temperature conditions with that after rapid quenching from equilibrium states to room temperature, one may examine the effectiveness of defect retention upon cooling. Several investigations of the defect structure using electrical transport measurements have been made on CdSe samples annealed at elevated temperatures and definite component pressures with subsequent measurement after quenching.

Borsenberger, Stevenson and Burmeister (*3*) measured the electron concentration as a function of Cd pressure on single crystal CdSe samples annealed at 800°C and then quenched to room temperature; their results are included in Fig. 9. This figure also includes measurements made at equilibrium conditions on a sample taken from the same boule. Although the 800°C isotherm exhibits the 1/3 Cd pressure dependence, the 648 and 604°C isotherms are essentially pressure independent. If the defect state is preserved with quenching, the slopes of equilibrium and quenched isotherms would be identical with possible displacement of the latter to lower electron concentrations since the donors may not be fully ionized at room temperature. Inasmuch as the observed pressure exponents (1/3 for equilibrium and about 0.1 for quenched isotherms, respectively) are different, it is concluded that the defect structure in CdSe is not preserved upon quenching. This lends further support to the observed rapid relaxation times and associated large interdiffusion coefficients for the electrically active native defects discussed in section, Discussion—Relaxation Times; the quench was probably less than 100 sec in which time the defect structure was altered by out-diffusion, precipitation or association.

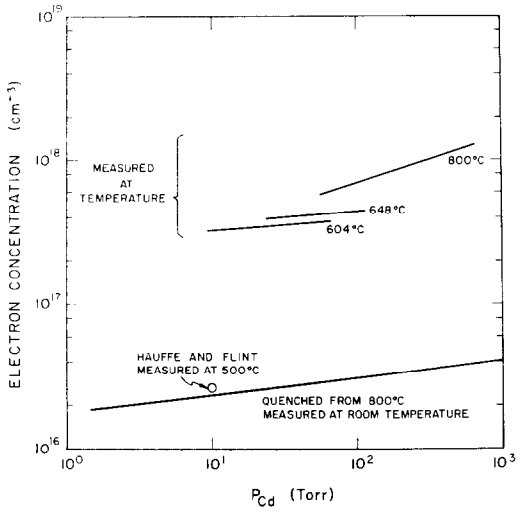

FIG. 9. The electron concentration as a function of Cd vapor pressure for CdSe measured at temperature (this investigation), measured at 500°C (*17*), and measured at room temperature after quenching from 800°C (*3*).

Since the slope of the isotherm for the quenched sample is approximately the same as the 604 and 648°C equilibrium isotherms, the quenched-in defect state is suggested to be representative of some temperature considerably less than 800°C, and to be dominated by impurity donors. The electrical behavior for this sample below 735°C is explained by the presence of a moderately high concentration of donor impurities. The magnitude of the electron concentrations for the quenched-in isotherm is substantially lower than the equilibrium isotherm, by approximately a factor of 30.

Hung, Ohashi and Igaki (*2*) also made room temperature electrical transport measurements on single crystal CdSe samples which had been annealed at 750 and 920°C (for 40–150 hr) under various component pressures and subsequently quenched. They reported that the purity of the materials used for crystal growth affected the results. Crystals prepared from 5-nine pure Cd and Se appeared to exhibit a Cd pressure exponent of 1/3 for the electron concentration; whereas, when 6-nine Cd and 5-nine Se were used, the electron concentration did not vary with P_{Cd}. These results were explained by the authors as follows: impurity donors and acceptors in the 5-nine Cd samples are in comparable concentrations and compensate one another; the native donor defect (assumed to be a doubly ionized Se vacancy) is present in concentrations greater than the uncompensated impurities and therefore dominates. For the 6-nine Cd samples fewer compensating acceptor impurities are present and hence donor impurities dominate over the native donors.

We suggest that the behavior described above

for both samples is not indicative of native defects in accord with the following comments:

1. The scatter in experimental data for those samples prepared from the "impure Cd" was such that it is not obvious that a 1/3 pressure exponent results;
2. Samples of both types were observed to have identical electron concentrations for annealing at the two temperatures over the range of pressures studied. Native donor concentrations are dependent on temperature.
3. One would expect native donors to dominate in those specimens prepared from the more pure starting materials.

Hauffe and Flint (*17*) measured the conductivity of polycrystalline sintered CdSe samples as a function of Cd pressure over a wide range of pressures between 300 and 500°C. At 500°C the measurements were made over the cadmium pressure range from $\sim 10^{-8}$ to ~ 10 Torr. Because of the difference in sample character when compared to the present study, a quantitative comparison is not meaningful. Furthermore, most of the data in the Hauffe and Flint study refer to lower cadmium pressures than in the present one. For purposes of qualitative comparison, however, the data point lying in the Cd pressure range in this study is included in Fig. 9. The conductivity reported in their study was converted to an electron concentration with a mobility taken from Fig. 3.

Conclusions

The results of high-temperature electrical transport measurements on CdSe in Cd-rich atmospheres have led to the following conclusions:

1. The dominant electrically active defect species above 650°C in undoped material are electrons and doubly ionized native donors, either Cd interstitials or Se vacancies.
2. At temperatures below 650°C, the decrease in Cd pressure exponent for electrons is attributed to the presence of residual electrically active donor impurities. The impurities Cu and In both exhibit donor behavior at elevated temperatures. Modification of the two species electroneutrality condition to include impurity donors permitted calculation of ionized impurity concentrations and the native donor incorporation constant; the activation energy for this latter quantity is 1.90 eV.
3. Defect structures, as suggested by electrical transport measurements and Cd self-diffusion measurements, are incongruous if one assumes the predominance of a single defect for the latter process.
4. Very short conductivity relaxation times were observed after stepwise changes in component pressure, suggesting relatively large interdiffusion coefficients.
5. The Hall mobilities measured between 200 and 800°C compared favorably with theoretical values calculated from optical mode and acoustic mode contributions, assuming a deformation potential of 12 eV for the latter.
6. Comparison between the high temperature electrical properties of CdSe measured at equilibrium and after quenching to room temperature leads to the conclusion that the native defect state is not retained upon cooling and that impurity donors dominate at room temperature.

Acknowledgment

The authors thank Dr. T. L. Larsen for helpful discussions during the course of the research and for critically reviewing the manuscript. This research was supported by the Atomic Energy Commission under contract AT(04-3)-326-PA 25, with partial support from the Advanced Research Projects Agency through the Center for Materials Research at Stanford University.

Appendix

The incorporation and ionization reactions and associated law of mass action expressions for Cd interstitials are as follows:

$$\mathrm{Cd(v)} \rightleftarrows \mathrm{Cd_i^x}; \quad K_{\mathrm{Cd}} = \frac{[\mathrm{Cd_i^x}]}{P_{\mathrm{Cd}}} \tag{A.1}$$

$$\mathrm{Cd_i^x} \rightleftarrows \mathrm{Cd_i^{\cdot}} + \mathrm{e'}; \quad K_1 = \frac{[\mathrm{Cd_i^{\cdot}}]n}{[\mathrm{Cd_i^x}]} \tag{A.2}$$

$$\mathrm{Cd_i^{\cdot}} \rightleftarrows \mathrm{Cd_i^{\cdot\cdot}} + \mathrm{e'}; \quad K_2 = \frac{[\mathrm{Cd_i^{\cdot\cdot}}]n}{[\mathrm{Cd_i^{\cdot}}]} \tag{A.3}$$

Similarly, for Cd vacancies:

$$\mathrm{CdSe(s)} \rightleftarrows V_{\mathrm{Cd}}^x + \mathrm{Cd(v)}; \quad K_V = [V_{\mathrm{Cd}}^x]P_{\mathrm{Cd}} \tag{A.4}$$

$$V_{\mathrm{Cd}}^x \rightleftarrows V_{\mathrm{Cd}}' + \mathrm{e^{\cdot}}; \quad K_3 = \frac{[V_{\mathrm{Cd}}']p}{[V_{\mathrm{Cd}}^x]} \tag{A.5}$$

$$V_{\mathrm{Cd}}' \rightleftarrows V_{\mathrm{Cd}}'' + \mathrm{e^{\cdot}}; \quad K_4 = \frac{[V_{\mathrm{Cd}}'']p}{[V_{\mathrm{Cd}}']} \tag{A.6}$$

TABLE II

THE DEPENDENCE OF POINT DEFECT CONCENTRATIONS IN CdSe ON THE Cd VAPOR PRESSURE FOR TWO DIFFERENT ELECTRONEUTRALITY CONDITIONS

	Defect and electron species concentrations						
Electroneutrality condition	$[Cd_i^x]$	$[Cd_i^{\cdot}]$	$[Cd_i^{\cdot\cdot}]$	$[V_{Cd}^x]$	$[V_{Cd}']$	$[V_{Cd}'']$	n
$n=[Cd_i^{\cdot}]$	$K_{Cd}P_{Cd}$	$K_{Cd_1}^{1/2}P_{Cd}^{1/2}$	K_2	$K_V P_{Cd}^{-1}$	$K_{Cd_1}^{1/2}K_{V_1}P_{Cd}^{-1/2}$	$K_{Cd_1}K_{V_2}$	$K_{Cd_1}^{1/2}P_{Cd}^{1/2}$
$n=2[Cd_i^{\cdot\cdot}]$	$K_{Cd}P_{Cd}$	$\frac{(K_{Cd_1})^{2/3}}{(2K_2)^{1/3}}P_{Cd}^{2/3}$	$\left(\frac{K_{Cd_2}}{4}\right)^{1/3}P_{Cd}^{1/3}$	$K_V P_{Cd}^{-1}$	$K_{V_1}(K_{Cd_2})^{1/3}P_{Cd}^{-2/3}$	$K_{V_1}(2K_{Cd_2})^{2/3}P_{Cd}^{-1/3}$	$(2K_{Cd_2})^{1/3}P_{Cd}^{1/3}$

In addition, for the creation of an electron-hole pair,

$$0 \rightleftarrows e' + e^{\cdot}; \quad K_i = np. \tag{A.7}$$

Assuming either of the two electroneutrality conditions,

$$n = [Cd_i^{\cdot}] \tag{A.8}$$

or

$$n = 2[Cd_i^{\cdot\cdot}] \tag{A.9}$$

enables the solution for the various defect and charge-carrier concentrations; these are tabulated in Table II. For the purpose of simplification, the following substitutions have been made in this table:

$$K_{Cd_1} = K_{Cd}K_1 \tag{A.10}$$

$$K_{Cd_2} = K_{Cd}K_1K_2 \tag{A.11}$$

$$K_{V_1} = \frac{K_V K_3}{K_i} \tag{A.12}$$

$$K_{V_2} = \frac{K_V K_3 K_4}{K_i^2}. \tag{A.13}$$

References

1. H. TUBOTA, H. SUZUKI, AND K. HIRAKAWA, *J. Phys. Soc. Jap.* **15**, 1701 (1960).
2. M. P. HUNG, N. OHASHI, AND K. IGAKI, *Jap. J. Appl. Phys.* **8**, 652 (1969).
3. P. M. BORSENBERGER, D. A. STEVENSON, AND R. A. BURMEISTER, *in* "International Conference on II–VI Semicond. Compounds" (D. G. Thomas, Ed.), p. 439, Benjamin, New York (1967).
4. K. R. ZANIO, *J. Appl. Phys.* **41**, 1935 (1970).
5. R. A. BURMEISTER AND D. A. STEVENSON, *Phys. Status Solidi* **24**, 683 (1967).
6. D. G. THOMAS AND E. A. SADOWSKI, *J. Phys. Chem. Solids* **25**, 395 (1964).
7. C. Z. VAN DOORN, *Rev. Sci. Instrum.* **32**, 755 (1961).
8. F. T. J. SMITH, *Solid State Commun.* **8**, 263 (1970).
9. H. H. WOODBURY AND R. B. HALL, *Phys. Rev. Lett.* **17**, 1093 (1966).
10. K. W. BÖER, R. BOYN, AND O. GOEDE, *Phys. Status Solidi* **3**, 1684 (1963).
11. R. BOYN, O. GOEDE, AND S. KUSCHNERUS, *Phys. Status Solidi* **12**, 57 (1965).
12. V. KUMAR AND F. A. KRÖGER, *J. Solid State Chem.* **3**, 406 (1971).
13. R. C. WHELAN AND D. SHAW, *Phys. Status Solidi* **29**, 145 (1968).
14. F. T. J. SMITH, *Met. Trans.* **1**, 617 (1970).
15. D. J. HOWARTH AND E. H. SONDHEIMER, *Pro. Roy. Soc., Ser. A* **219**, 53 (1953).
16. J. BARDEEN AND W. SHOCKLEY, *Phys. Rev.* **80**, 72 (1950).
17. K. HAUFFE AND H. G. FLINT, *Ann. Phys.* **15**, 141 (1955).
18. L. C. GREENE, D. C. REYNOLDS, S. J. CZYZAK, AND W. M. BAKER, *J. Chem. Phys.* **29**, 1375 (1958).